

# Energy-Efficient Time Synchronization Based on Asynchronous Source Clock Frequency Recovery and Reverse Two-Way Message Exchanges in Wireless Sensor Networks

Kyeong Soo Kim, *Member, IEEE*, Sanghyuk Lee, and Eng Gee Lim, *Member, IEEE*

**Abstract**—We consider energy-efficient time synchronization in a wireless sensor network where a head node (i.e., a gateway between wired and wireless networks and a center of data fusion) is equipped with a powerful processor and supplied power from outlet, and sensor nodes (i.e., nodes measuring data and connected only through wireless channels) are limited in processing and battery-powered. It is this *asymmetry* that our study focuses on; unlike most existing schemes to save the power of all network nodes, we concentrate on battery-powered sensor nodes in minimizing energy consumption for time synchronization. We present a time synchronization scheme based on asynchronous source clock frequency recovery and reverse two-way message exchanges combined with measurement data report messages, where we minimize the number of message transmissions from sensor nodes, and carry out the performance analysis of the estimation of both measurement time and clock frequency with lower bounds for the latter. Simulation results verify that the proposed scheme outperforms the schemes based on conventional two-way message exchanges with and without clock frequency recovery in terms of the accuracy of measurement time estimation and the number of message transmissions and receptions at sensor nodes as an indirect measure of energy efficiency.

**Index Terms**—Time synchronization, energy efficiency, source clock frequency recovery, two-way message exchanges, wireless sensor networks.

## I. INTRODUCTION

A common time frame among network nodes in a wireless sensor network (WSN) is critical for their carrying out important operations like fusing data from different sensor nodes, time-based channel sharing and media access control (MAC) protocols, and coordinated sleep wake-up node scheduling mechanisms [1]. In a typical WSN, a head/master node (i.e., a base station that serves as a gateway between wired and wireless networks and a center for fusion of data from distributed sensors) is equipped with a powerful processor and supplied power from outlet, while sensor/slave nodes (i.e., nodes measuring data with sensors and connected to a WSN only through wireless channels) are limited in processing and battery-powered. It is this *asymmetry* that our study focuses on; unlike most existing schemes trying to save the power of all network nodes (e.g., [2] and [3]), we concentrate on battery-powered sensor nodes, which are

many in number, in minimizing energy consumption for time synchronization.

In this paper we mean by *time synchronization* a process of establishing a common time frame with which the nodes in a network can operate one another, whether their clocks are synchronized or not. By *clock synchronization*, on the other hand, we mean a process of synchronizing each node clock to that of a common reference node, typically through a logical clock that is a function of a physical clock, which is one way of achieving time synchronization. Note that without synchronizing node clocks, we can still provide a common time frame for the operation of network nodes. For instance, in multi-hop extension of the reference broadcast synchronization (RBS) algorithm [4], there are multiple broadcast domains independently maintaining their own clocks. In this case, the common time frame among multiple broadcast domains is provided through time conversion at gateway nodes belonging to neighboring domains.

In the literature, time synchronization is formulated as the problem of estimating clock parameters, often including node distances, in a pairwise (distributed) or a network-wide (global) manner [5]–[8]. Few works, however, have focused on the mode of operation (i.e., time vs. clock synchronization discussed above) and the way of implementation related with energy efficiency. To achieve better performance, several joint estimation algorithms for both clock parameters and pair-wise distances have been proposed (e.g., [7] and [6]). Most of them are, however, based on centralized and global offline algorithms, and the estimation of parameters and the way of implementing clock/time synchronization together with the delivery of the results of estimation are not explicitly discussed. While joint estimation algorithms usually assume that all sensor nodes are available in the beginning, recursive and online operation of synchronization schemes are critical for WSN applications because there are nodes who join later or resume their operations in the middle.

In this paper we present an energy-efficient time synchronization scheme based on asynchronous source clock frequency recovery (SCFR) [9] and *reverse* two-way message exchanges combined with measuring data report messages, where we minimize the number of message transmissions and receptions at sensor nodes, especially the number of message transmissions noting that the energy for message transmission is typically higher than that for message reception [10]. In the proposed time synchronization scheme, only the frequency of a sensor node clock is synchronized to that of the reference clock at the head node, but not its clock offset; the proposed scheme is based on the idea of the separation of the clock

This work was supported in part by Xi'an Jiaotong-Liverpool University Centre for Smart Grid and Information Convergence (CeSGIC) and Research Development Fund (under Grant RDF-14-01-25). An earlier version of this paper was presented in part at ICISCA 2015, Kuala Lumpur, Malaysia, June 2015, and ISAE 2015, Busan, Korea, October 2015.

K. S. Kim, S. Lee, and E. G. Lim are with the Department of Electrical and Electronic Engineering, Xi'an Jiaotong-Liverpool University, Suzhou 215123, Jiangsu Province, P. R. China (e-mail: {Kyeongsoo.Kim, Sanghyuk.Lee, Enggee.Lim}@xjtlu.edu.cn).

frequency<sup>1</sup> estimation/compensation at sensor nodes and the clock offset and delay estimation at the head node. For the clock frequency recovery, each sensor node passively listens to any messages with timestamps either broadcasted (e.g., beacons) or unicast (e.g., control messages to a specific node) from the head node and carries out asynchronous source clock frequency recovery described in [9], which is basically one-way clock frequency estimation. For the clock offset and delay estimation, a simple two-way message exchange procedure [11], [12] is used but in a reverse direction where the head node initiates the procedure and keeps track of the offsets between its reference clock and sensor node clocks; also, instead of dedicated, periodical synchronization message exchanges, we embed the synchronization “Response” messages of the two-way message exchange procedure in the measurement data report messages from sensor nodes in order to minimize the number of message transmissions. In this way we can move most of time synchronization operations to the head node and reduce the complexity and thereby power consumption of sensor nodes for time synchronization. To carry out usual WSN operations with the proposed time synchronization scheme, the head node translates timestamp values based on clock offset information before transmitting control messages to sensor nodes.

The major contributions of this work are three-fold: First, it provides a new energy-efficient time synchronization scheme for asymmetric WSNs to minimize the number of two-way message exchanges by cleverly combining one-way clock skew estimation/compensation and reverse two-way message exchanges. Note that the two-way message exchanges cannot be avoided in estimating both clock offset and clock skew because it is impossible to separate the effects of clock offset and propagation delay with one-way message exchanges alone [1], [13]. The proposed scheme does not only minimize the number of two-way message exchanges but also enable the use of simple, low-complexity one-way clock skew estimation/compensation algorithms to avoid the high complexity of advanced estimation algorithms taking into nuisance parameters like mean and variance of the propagation delay. Secondly, we formally describe the operations of and analyze the time synchronization performance of the proposed scheme: By separately modeling times of a hardware clock and a logical clock at a network node, we can capture the dynamic nature of the proposed time synchronization scheme in the analysis, which estimates clock parameters of a counterpart and updates its own logical clock recursively. Thirdly, we also analyze the performance of measurement time estimation based on both conventional and reverse two-way message exchanges. As for clock skew estimation/compensation, we carry out a comparative analysis of the performance of one-way and two-way maximum likelihood (ML) and ML-like estimators and derive Cramér-Rao lower bounds and lower bounds for ML and ML-like estimators, respectively.

The rest of the paper is organized as follows: In Section II, we describe the proposed time synchronization scheme with

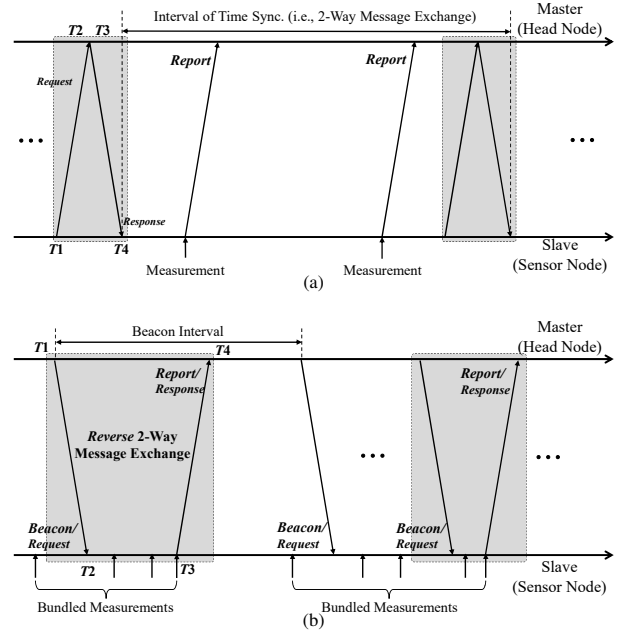


Fig. 1. Comparison of two-way message exchanges: (a) Conventional two-way message exchanges as in the time-sync protocol for sensor networks (TPSN) [12]; (b) reverse two-way message exchanges of the proposed scheme shown with optional bundling of measurements in a “Report/Response” message.

hardware and logical clock models; we also analyze the effect of clock skew on measurement time estimation in both conventional and reverse two-way message exchanges, present joint ML and ML-like one-way clock skew estimators with their performance bounds, and discuss an extension to multi-hop time synchronization through gateway nodes. Section III presents the results of simulations for a comparative analysis of the performance of one-way and two-way clock skew estimators for asynchronous SCFR and the investigation of the time synchronization performance and the energy efficiency of the proposed scheme compared to the schemes based on conventional two-way message exchanges with and without SCFR. Section IV reviews the related work in comparison to our work before concluding this paper in Section V.

## II. ENERGY-EFFICIENT TIME SYNCHRONIZATION FOR ASYMMETRIC WSNs

The major idea of the proposed scheme is to allow independent, unsynchronized slave clocks at sensor nodes but running at the same frequency as the reference clock at a head node through the asynchronous SCFR described in [9], which needs only the reception of messages with timestamps at sensor nodes. The clock offset, on the other hand, is estimated at the head node based on the reverse two-way message exchanges. Fig. 1 illustrates this idea in comparison to conventional two-way message exchanges.

First, the proposed scheme shown in Fig. 1 (b) does not have periodic, dedicated two-way message exchanges with synchronization messages like “Request” and “Response” shown in Fig. 1 (a); instead, the “Request” and “Response” messages

<sup>1</sup>We use the terms “clock frequency” and “clock skew” interchangeably in this paper.

<b>Response Message</b> (timestamps $T_1, T_2, T_3$ , sequence number of the latest Request message, ...)	<b>Measurement Data + Timestamp #1</b>	...	<b>Measurement Data + Timestamp #N</b>
--	--	-----	--

Fig. 2. Payload structure of a "Report/Response" message of the proposed scheme with optional bundling of measurement data and timestamps.

are embedded in the most recent timestamped message—either broadcasted or unicasted to a specific node—from the head node and a measurement data report message from a sensor node, respectively. When there are no strict timing requirements for the processing of measurement data, the measurement data and their corresponding timestamps can be optionally bundled together in a "Report/Response" message, whose payload structure is shown in Fig. 2, in order to further reduce the number of message transmissions; in this case the clock offset estimated based on the timestamp of the last measurement data #N is collectively applied to all bundled measurement data in estimating their occurrences with respect to the reference clock at the head node.

Secondly, the direction of two-way message exchanges of the proposed scheme is reversed, i.e., it is the master (i.e., the head node) that sends the "Request" messages, not the slave (i.e., the sensor node), unlike the conventional two-way messages exchanges; as a result, the master knows the current status of the slave clock, but the slave does not. So the information of slave clocks (i.e., clock offsets with respect to the reference clock) is centrally managed at the head node.

For operations like coordinated sleep wake-up node scheduling, before sending a control message, the head node first adjusts the time for future operation based on the clock offset of the recipient sensor node. In this way, even though sensor nodes in the network have clocks with different clock offsets, their operations can be coordinated based on the common reference clock at the head node.

#### A. Hardware and Logical Clock Models

We consider an asymmetric WSN where one head (master) node and  $N$  sensor (slave) nodes all equipped with independent hardware clocks based on quartz crystal oscillators. For simplicity, we take time  $t$  of the head node clock as a global reference and describe times of slave hardware clocks as functions of  $t$ . We use the first-order affine clock model [6] to describe time  $T_i$  of the hardware clock at the  $i$ th sensor node as follows: For  $i \in [0, 1, \dots, N-1]$ ,

$$T_i(t) = (1 + \epsilon_i)t + \theta_i, \quad (1)$$

where  $(1 + \epsilon_i) \in \mathbb{R}_+$  and  $\theta_i \in \mathbb{R}$  are clock frequency ratio and clock offset, respectively. Note that  $\epsilon_i$  is called a clock skew in the literature, which is defined as a *normalized clock frequency difference* between hardware clocks, and its typical value for clocks based on quartz crystal oscillators is of the order of tens of ppm (i.e.,  $\epsilon_i \ll 1$ ).

WSN operations at a sensor node is based on a logical clock, whose time is again a function of the time of its physical clock and takes into account the adjustments by an adopted time synchronization scheme (e.g., offset adjustment by two-way message exchanges and frequency adjustment by SCFR).

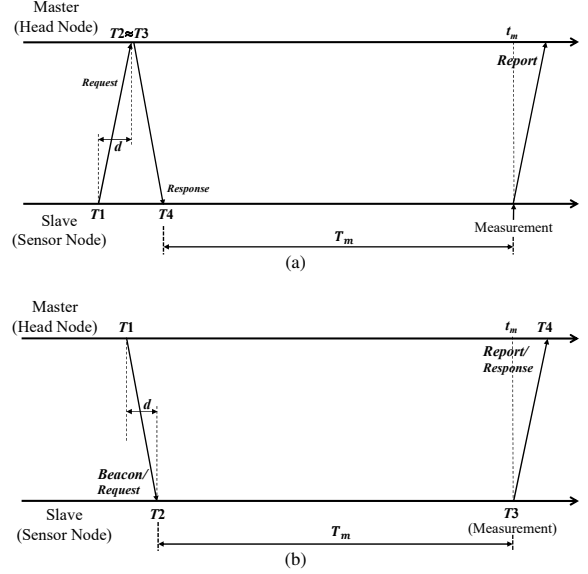


Fig. 3. Timing diagrams for the analysis of the measurement time estimation error: (a) Conventional two-way message exchanges; (b) reverse two-way message exchanges of the proposed scheme.

Specifically, time  $\mathcal{T}_i$  of the logical clock at the  $i$ th sensor node can be modeled as a piecewise linear function as follows<sup>2</sup>: For  $t_k < t \leq t_{k+1}$  ( $k=0, 1, \dots$ ),

$$\mathcal{T}_i(T_i(t)) = \mathcal{T}_i(T_i(t_k)) + \frac{T_i(t) - T_i(t_k)}{1 + \hat{\epsilon}_{i,k}} - \hat{\theta}_{i,k}, \quad (2)$$

where  $t_k$  is the reference time when a  $k$ th synchronization occurs, and  $\hat{\epsilon}_{i,k}$  and  $\hat{\theta}_{i,k}$  are the estimated clock skew and offset from the  $k$ th synchronization. If the synchronization is only for frequency, we set  $\hat{\theta}_{i,k}$  to 0 in (2); if the synchronization is only for offset, on the other hand, we set  $\hat{\epsilon}_{i,k}$  to 0 in (2). It should be noted that  $\mathcal{T}_i$  in (2) is the function of  $T_i(t)$ , but not  $t$  itself, because the reference time  $t$  is not known at a sensor node and the only available time is from a local hardware clock (i.e.,  $T_i(t)$ ).

#### B. Effect of Clock Skew on Measurement Time Estimation

Here we compare the effect of clock skew on the measurement time estimation in both conventional and reverse two-way message exchange procedures by an approximate analysis of the best-case performance under a deterministic delay (i.e., no random component) and no bundled measurements. Fig. 3 shows timing diagrams for the analysis of the measurement time estimation error, where we assume the same amount of time difference  $T_m$  between the measurement occurrence and the reception of the last time synchronization message—i.e., the "Response" message for the conventional two-way message exchanges and a beacon ("Request") message for the reverse two-way message exchanges.

Because MAC-layer timestamping of messages can remove all the sources of uncertainties except the propagation delay [2]

<sup>2</sup>This model fits for WSN operations requiring times of discrete events only. More complicated (often nonlinear) models, however, is better suited for applications like playback of multimedia streaming where an analog or digital phase-locked loop (PLL) is used to generate a clock signal [9].

and the variation in propagation delays is negligible in single-hop transmissions, the clock offset estimation error  $\Delta\hat{\theta}_i$  in the two-way message exchanges without clock skew compensation (i.e., based on the hardware clock model in (1)) is given by [12]

$$\Delta\hat{\theta}_i = \frac{(T_4 - T_1)\epsilon_i}{2} = d \times \epsilon_i, \quad (3)$$

where  $d$  denotes one-way propagation delay. The measurement time estimation error for the conventional two-way message exchanges shown in Fig. 3 (a), therefore, can be expressed as

$$\Delta\hat{t}_m^{Conv.} = d\epsilon_i + T_m\epsilon_i = (d + T_m)\epsilon_i. \quad (4)$$

If  $T_m \gg d$ , the measurement time error can be approximated as

$$\Delta\hat{t}_m^{Conv.} \sim T_m \times \epsilon_i. \quad (5)$$

When the clock skew is compensated, (5) becomes

$$\Delta\hat{t}_m^{Conv.} \sim T_m \times \Delta\hat{\epsilon}_i, \quad (6)$$

where  $\Delta\hat{\epsilon}_i$  is the clock skew estimation error.

For the reverse two-way message exchanges shown in Fig. 3 (b), because the ‘‘Request’’ message of the reverse two-way message exchanges is embedded in the measurement data ‘‘Report’’ message from a sensor node as shown in Fig. 2, there is no time difference between the measurement time and the end of two-way message exchange (i.e.,  $T_4$ ). In this case the two-way message exchange procedure is the only source of error, i.e.,

$$\Delta\hat{t}_m^{Rev.} = \frac{(T_4 - T_1)\Delta\hat{\epsilon}_i}{2} = \frac{(2d + T_m)\Delta\hat{\epsilon}_i}{2}. \quad (7)$$

Again, if  $T_m \gg d$ , the measurement time estimation error can be approximated as

$$\Delta\hat{t}_m^{Rev.} \sim \frac{T_m}{2} \times \Delta\hat{\epsilon}_i. \quad (8)$$

From (6) and (8), we can see that, when being isolated from the effect of random component of delay, the proposed scheme can reduce the effect of clock skew on the measurement time estimation error by a factor of two for  $T_m \gg d$ . Because the time difference  $T_m$  between the reception of the last beacon (or any timestamped message) from the head node and the measurement occurrence at the sensor node can be a larger value in practice, however, it is still important to compensate the clock skew at sensor nodes in the proposed scheme.

### C. Asynchronous SCFR at Sensor Nodes: One-Way Clock Skew Estimation

One of the essential components of the proposed time synchronization scheme is the recovery of the reference clock frequency at sensor nodes based on one-way message dissemination from the head node. Once we estimate the clock skew  $\epsilon_i$  in (1), the reference clock frequency can be recovered through the clock skew compensation of the logical clock model in (2).

In case of two-way message exchanges, both joint ML estimation of clock offset and skew with a known fixed portion of delay and separate ML-like estimation of clock skew are studied in [14]. As for one-way message dissemination, here

we derive both joint ML and separate ML-like estimators in a similar manner but based on the problem formulation in [9].

Let  $t_d(k)$  ( $k=0, 1, \dots$ ) be the reference time for the  $k$ th message’s departure from the head node; note that  $t_d(k)$  also denotes the value of the timestamp carried by the  $k$ th message. From the hardware clock model in (1), we can obtain  $t_{a,i}(k)$ , the arrival time of the  $k$ th message with respect to the  $i$ th sensor node’s *hardware clock*, as follows:

$$\begin{aligned} t_{a,i}(k) &= T_i(t_d(k)) + d(k) \\ &= (1 + \epsilon_i)t_d(k) + \theta_i + d(k), \end{aligned} \quad (9)$$

where  $d(k)$  denotes a one-way packet delay from the head node to the  $i$ th sensor node in terms of the  $i$ th sensor node’s hardware clock.<sup>3</sup> For the observation of timestamps from (9), we can obtain the joint ML estimators (MLEs) of clock offset and skew as stated in Proposition 1.

*Proposition 1:* For a white Gaussian delay  $d(k)$  with known mean  $d$  and variance  $\sigma^2$ , the joint ML estimators (MLEs) for clock offset  $\hat{\theta}_i^{ML}(k)$  and skew  $\hat{R}_i^{ML}(k)$  in (9) are given by

$$\hat{\theta}_i^{ML}(k) = \frac{\overline{t_d^2} \cdot \overline{t_{a,i}} - \overline{t_d} \cdot \overline{t_d t_{a,i}}}{\overline{t_d^2} - (\overline{t_d})^2} - d, \quad (10)$$

$$\hat{R}_i^{ML}(k) = \frac{\overline{t_d t_{a,i}} - \overline{t_d} \cdot \overline{t_{a,i}}}{\overline{t_d^2} - (\overline{t_d})^2}, \quad (11)$$

where the notations  $\overline{x}$  and  $\overline{xy}$  denote the average values of  $x(j)$  (i.e.,  $\sum_{j=0}^k x(j)/k$ ) and  $x(j)y(j)$  (i.e.,  $\sum_{j=0}^k x(j)y(j)/k$ ), respectively. Also  $\hat{\theta}_i^{ML}(k)$  and  $\hat{R}_i^{ML}(k)$  are *efficient estimators* [16, p. 34] which are unbiased and attain the Cramér-Rao lower bounds (CRLBs) given by

$$\text{Var}(\hat{\theta}_i(k)) \geq \frac{\sigma^2 \cdot \overline{t_d^2}}{k \left\{ \overline{t_d^2} - (\overline{t_d})^2 \right\}}, \quad (12)$$

$$\text{Var}(\hat{R}_i(k)) \geq \frac{\sigma^2}{k \left\{ \overline{t_d^2} - (\overline{t_d})^2 \right\}}. \quad (13)$$

*Proof:* The proof of Proposition 1 is presented in Appendix A. ■

Note that, even though the mean and the variance of white Gaussian delay are assumed to be known for the derivation of the joint MLEs, the resulting clock skew estimator  $\hat{R}_i^{ML}(k)$ —the only one needed in the proposed scheme—does not depend on it.

Compared to the joint MLEs for two-way message exchanges derived in [14], (10) and (11) take simpler expressions, but they are still complicated and not suitable for recursive implementation. Because we are only interested in the estimation of the clock skew—equivalently the ratio of clock frequencies—at sensor nodes, we can formulate the estimation problem where the clock skew is the only parameter to estimate. In [9], the problem of asynchronous SCFR is formulated as a linear *regression through the origin (RTO)*

<sup>3</sup>This definition of the one-way delay (i.e., in terms of the sensor nodes’ hardware clock) is different from that in [14] and [15], where the delay is defined in terms of the head node clock, and makes simpler the derivation of the one-way estimators in this paper.

model by subtracting both sides of (9) with their initial values: For  $k = 1, 2, \dots$ ,

$$\tilde{t}_{a,i}(k) = (1 + \epsilon_i)\tilde{t}_d(k) + \tilde{d}(k), \quad (14)$$

where  $\tilde{t}_{a,i}(k) \triangleq t_{a,i}(k) - t_{a,i}(0)$ ,  $\tilde{t}_d(k) \triangleq t_d(k) - t_d(0)$ , and  $\tilde{d}(k) \triangleq d(k) - d(0)$ . Note that  $\tilde{d}(k)$  now represents a noise process with a zero mean for a stationary delay model.

Note that  $\tilde{t}_{a,i}(k)$ 's in (14) are not independent one another due to  $\tilde{d}(k)$ . The derivation of an MLE based on all observations of  $\tilde{t}_{a,i}(k)$ 's, therefore, is not straightforward. In [9], two practical estimators are proposed in this regard, i.e., the recursive least squares (RLS) and the cumulative ratio (CR), which are not based on any assumption on the delay distribution. Of the two estimators, the CR estimator is best suited for battery-powered sensor nodes in the proposed time synchronization scheme due to its lower complexity. If we define  $R_i$  as the ratio of the  $i$ th sensor node hardware clock frequency to that of the reference clock (i.e.,  $1 + \epsilon_i$ ), the CR estimator  $\hat{R}_i^{CR}(k)$  is given by

$$\hat{R}_i^{CR}(k) = \frac{\tilde{t}_{a,i}(k)}{\tilde{t}_d(k)}. \quad (15)$$

From (14), we can see that  $\hat{R}_i^{CR}(k)$  can be rewritten as follows:

$$\hat{R}_i^{CR}(k) = R_i + \frac{\tilde{d}(k)}{\tilde{t}_d(k)}, \quad (16)$$

where its noise component becomes zero as time goes to infinity irrespective of its statistical characteristics. Unlike the RLS estimator, there are no design parameter values or initial values to set for the CR estimator.

Note that for a Gaussian delay model, the CR estimator becomes an unbiased estimator achieving its lower bound as stated in Proposition 2.

*Proposition 2:* For a white Gaussian delay  $\tilde{d}(k)$  with zero mean and variance  $\sigma^2$ , the CR estimator in (16) becomes an *unbiased estimator* which attains the lower bound<sup>4</sup> given by

$$\text{Var}\left(\hat{R}_i^{CR}(k)\right) \geq \frac{2\sigma^2}{\tilde{t}_d(k)^2}.$$

*Proof:* The proof of Proposition 2 is presented in Appendix B. ■

#### D. Extension to Multi-Hop Time Synchronization

Fig. 4 shows how the proposed scheme can be extended to a hierarchical structure for network-wide, multi-hop synchronization through simple packet-relaying or more advanced time-translating gateway nodes, the latter of which act as both head nodes (for the nodes in the lower hierarchy) and normal sensor nodes (for the gateway node in the higher hierarchy): For example, consider the message transmission from the sensor node S to the head node through the two gateway nodes G1 and G2 as shown in Fig. 4. In case of *packet relay*, G2 simply passes the received timestamped message from S to G1 and G1 to the head node without any change of the

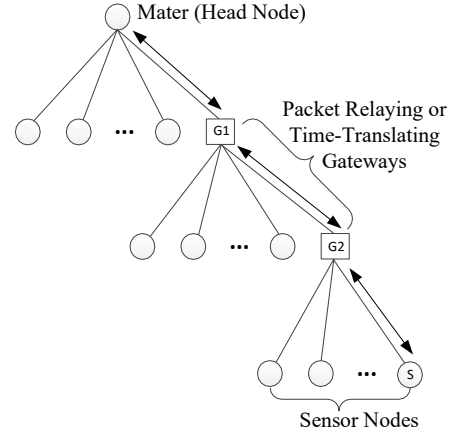


Fig. 4. Extension of the proposed time synchronization scheme to a hierarchical structure for network-wide, multi-hop synchronization through packet-relaying or time-translating gateway nodes.

value of timestamp in the middle. In case of *time translation*, because G2 acts as a head node for S, it first translates the value of timestamp based on the information on the clock offset of S. Then G2 relays the message from S to G1 with translated timestamp value (with respect to its own clock). From G1's point of view, G2 is just one of sensor nodes it manages. Again, based on the information on the clock offset of G2, G1 translates the value of clock offset with respect to its own clock and relays the message to the head node. Finally, the head node receives the message from S, which is just relayed by G1, and translates the timestamp value based on the information on the clock offset of G1 it manages. In this way the head node can obtain the measurement data and its occurrence in time reported by S with respect to its own reference clock.

It is clear that, compared to time-translating gateway nodes, packet-relaying gateway nodes could be much simpler because there is no additional functionality (i.e., estimation and management of the offset information and translation of timestamp values) except packet relaying. A downside, however, is that they introduce larger packet delays resulting from queueing and MAC operations, which could deteriorate the performance of time synchronization.

### III. SIMULATION RESULTS

We carry out a series of simulation experiments to investigate the performance of the proposed time synchronization scheme in terms of the accuracy of measurement time estimation and the number of message transmissions and receptions at a sensor node in comparison with those based on the conventional two-way message exchanges. We also analyze the performance of one-way clock skew estimators independently of the proposed time synchronization scheme to choose the best one for battery-powered sensor nodes.

For the simulations, we consider a simple WSN with one head node and one sensor node that are deployed 100 m from each other because the time synchronization of a sensor node in the proposed scheme can be carried out independently of that of other sensor nodes. As in [7], we set the clock

<sup>4</sup>This lower bound is in fact the CRLB for the case when the observations are limited to the timestamps from the first and last messages.

frequency ratio  $R_i$  and the clock offset  $\theta_i$  to  $1 + 100$  ppm and 1 s, respectively. We model propagation delay, which takes into account timestamp generation and reception noise as well, with an independent and identically distributed (i.i.d.) Gaussian process unless specified otherwise.

### A. Performance of One-Way Clock Skew Estimation

First, we analyze the performance of one-way clock skew estimators discussed in Section II-C, together with the two-way ML-like estimator for Gaussian delay model (GMLLE) proposed in [14] for comparison. Fig. 5 shows the mean square error (MSE) of both one-way and two-way clock skew estimators with Gaussian delays with standard deviation of 1 ns and 1  $\mu$ s, which are calculated over 10,000 simulation runs. Fig. 6 also shows the results with first-order autoregressive (AR(1)) random delays with correlation coefficient ( $\rho$ ) of 0.6 and standard deviation of 1  $\mu$ s and 1 ms; the results in this case demonstrate the performance of the estimators under correlated delays, which reflect the case of multi-hop extension through packet-relaying gateway nodes as discussed in Section II-D.

The results for both Gaussian and AR(1) delays show that the joint MLE provides the best performance as expected because it can use all observed timestamp values. The performance gap between the joint MLE and other one-way estimators (i.e., CR and RLS), however, becomes narrower when the delay does not follow the Gaussian distribution and has correlation. The estimation performance of the two-way scheme (i.e., GMLLE), on the other hand, is the worst *given the number of messages exchanged*, which indicates that the two-way message exchange procedure is not energy-efficient in estimating the clock skew only.

As discussed in Section II-C, due to its lower complexity and robustness to delay characteristics, we use the CR estimator at battery-powered sensor nodes in the investigation of the performance of the proposed time synchronization scheme in the following sections.

### B. Performance of Measurement Time Estimation and Energy Efficiency

For the analysis of the performance of the proposed time synchronization scheme, we run simulations for three different values of synchronization interval (SI)<sup>5</sup>—i.e., 100 s, 1 s and 10 ms—to investigate the effect of the time difference  $T_m$  between the last time synchronization message from the head node and the measurement occurrence at the sensor node. The propagation delay is modeled as an i.i.d. Gaussian process with a standard deviation of 1 ns. During the observation interval of 1 h, total 100 measurements are made where their corresponding data arrivals are modeled as a Poisson process. For SCFR, we use the CR estimator for the proposed scheme based on the observation in Section III-A and the GMLLE for the two-way scheme for comparison.

The results of SCFR at the sensor node and measurement time estimation at the head node (i.e., the estimation of the

<sup>5</sup>This is the interval of beacons for the proposed scheme and the interval of two-way message exchanges for others.

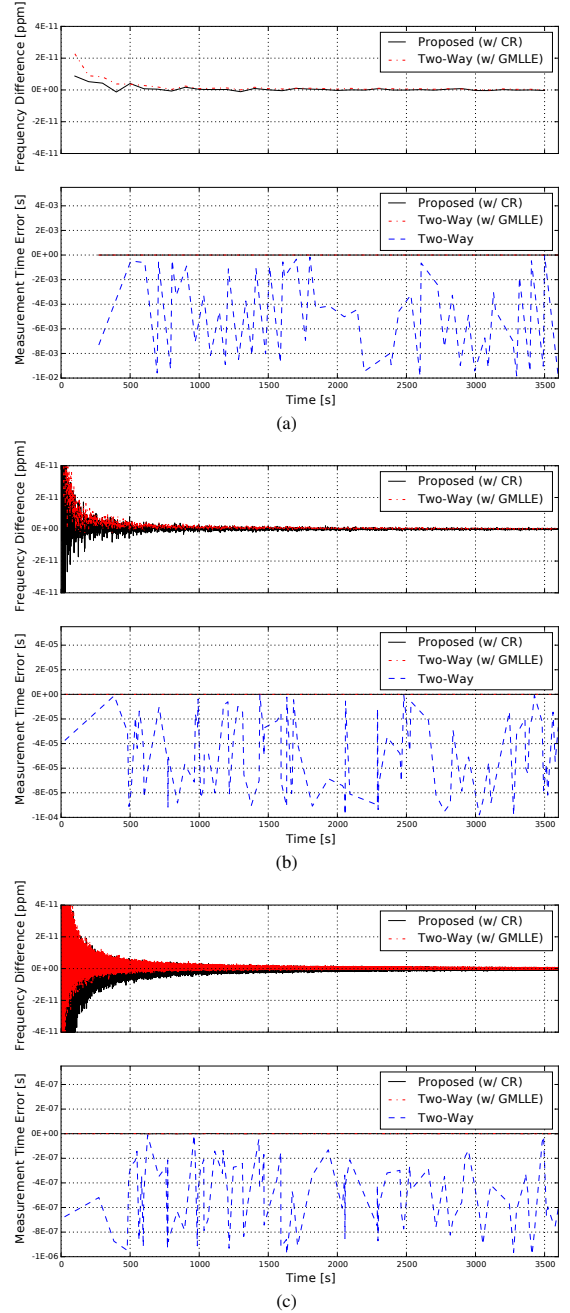


Fig. 7. Performance of SCFR at a sensor node and measurement time estimation at a head node for SI of (a) 100 s, (b) 1 s, and (c) 10 ms.

measurement time at the sensor node with respect to the reference clock at the head node) are shown in Fig. 7, and their MSEs calculated over samples from one simulation run with the number of message transmissions ( $N_{TX}$ ) and receptions ( $N_{RX}$ ) at the sensor node are summarized in Table I.

As shown by the approximate analysis in Section II-B, the results show that, without SCFR (i.e., “Two-Way”), the measurement time estimation errors highly depend on the synchronization interval. The use of SCFR (i.e., “Proposed (w/ CR)” and “Two-Way (w/ GMLLE)”), on the other hand, greatly reduces this dependency, and the resulting measurement time estimation errors (i.e., the square root of MSE of measurement

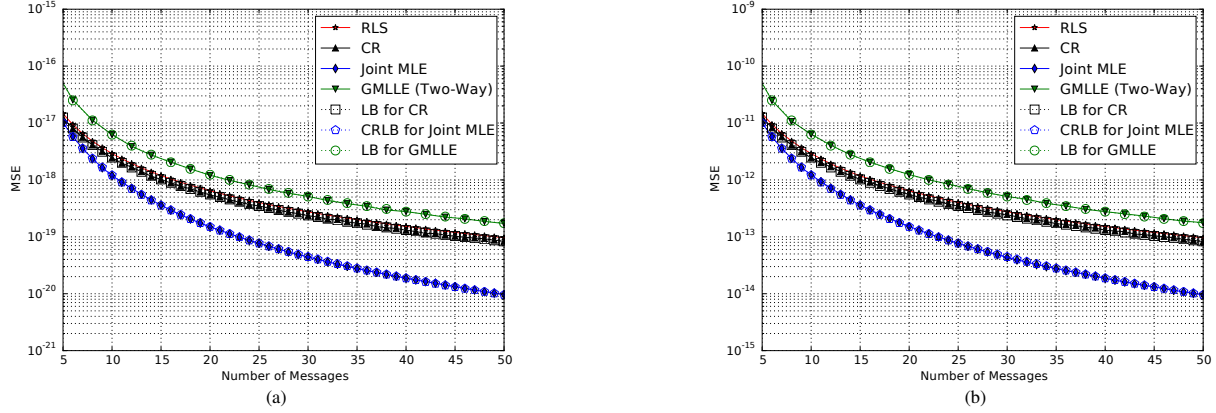


Fig. 5. MSE of the estimated clock skews from one-way and two-way clock skew estimators for Gaussian random delays with standard deviation ( $\sigma$ ) of (a) 1 ns and (b) 1  $\mu$ s.

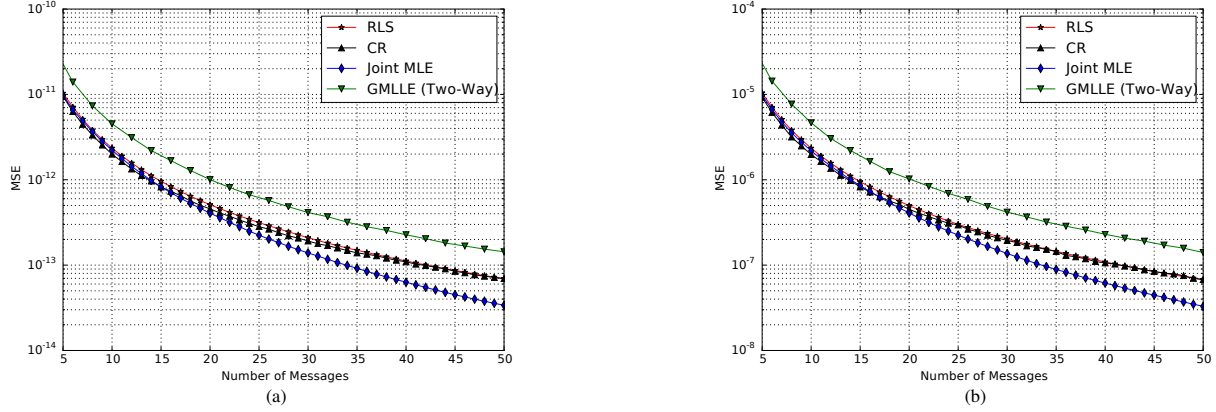


Fig. 6. MSE of the estimated clock skews from one-way and two-way clock skew estimators for AR(1) random delays with correlation coefficient ( $\rho$ ) of 0.6 and standard deviation of (a) 1  $\mu$ s and (b) 1 ms.

TABLE I  
RESULTS OF TIME SYNCHRONIZATION SIMULATIONS FOR DIFFERENT SIS

Synchronization Scheme		Skew Estimation MSE <sup>1</sup>	Measurement Time Estimation MSE <sup>1</sup>	$N_{TX}$	$N_{RX}$
Proposed	SI = 100 s	8.8811E-25	5.8990E-19	100	36
	SI = 1 s	9.1748E-25	5.4210E-19	100	3600
	SI = 10 ms	1.0887E-24	4.7684E-19	100	360100
Two-Way with GMLLE	SI = 100 s	1.9021E-24	4.7784E-19	136	36
	SI = 1 s	1.7034E-24	6.1452E-19	3700	3600
	SI = 10 ms	9.0992E-25	4.0485E-19	360100	360000
Two-Way	SI = 100 s	N/A	3.4900E-05	136	36
	SI = 1 s		3.4564E-09	3700	3600
	SI = 10 ms		3.3638E-13	360100	360000

<sup>1</sup> For the samples obtained from 360 s (i.e., one tenth of the observation period) to avoid the effect of a transient period.

time estimation) are of the order of the noise standard deviation (i.e., 1 ns) for all values of the synchronization interval, which means that the synchronization interval can be increased without much affecting the time synchronization performance to save energy. Table I also shows that the number of message transmissions for the proposed scheme is the same as the number of measurements irrespective of the synchronization interval, while the number of message receptions increases as the synchronization interval decreases for all the schemes considered; in case of the synchronization interval of 1 s, the number of message transmissions is 100 for the proposed

scheme and 3,700 (100 for the measurement data and 3,600 for the synchronization messages) for the schemes based on the conventional two-way messages exchanges.

### C. Effect of Bundling of Measurement Data

We also investigate the effect of the bundling of measurement data described in Section II with fixed synchronization interval of 1 s. Fig. 8 shows the measurement time estimation errors for different numbers of bundled measurements ( $N_{BM}$ ) in one “Report/Response” message, and again their MSEs calculated over samples from one simulation run with the

TABLE II  
RESULTS OF TIME SYNCHRONIZATION SIMULATIONS FOR DIFFERENT NUMBERS OF  
BUNDLED MEASUREMENTS ( $N_{BM}$ ) WITH SI OF 1 s.

Synchronization Scheme	Measurement Time Estimation MSE <sup>1</sup>	$N_{TX}$	$N_{RX}$
Proposed	$N_{BM} = 1$	100	3600
	$N_{BM} = 2$	50	3600
	$N_{BM} = 5$	20	3600
	$N_{BM} = 10$	10	3600

<sup>1</sup> For the samples obtained from 360 s (i.e., one tenth of the observation period) to avoid the effect of a transient period.

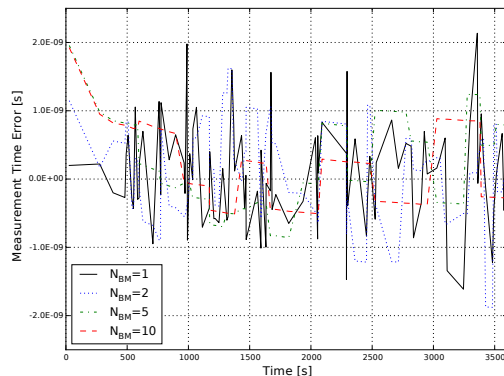


Fig. 8. Measurement time estimation errors for different numbers of bundled measurements ( $N_{BM}$ ) with SI of 1 s.

number of message transmissions and receptions at the sensor node are summarized in Table II.

It is evident from the figure and the table that the measurement time estimation errors are not much affected by the number of bundled measurements after the initial transient period (i.e., after around 500 s). In fact, the table shows that the MSE of measurement time estimation slightly decreases as the number of bundled measurements increases; this is because all the measurement data reported in a “Report/Response” message share the same estimated value of the clock offset as the last measurement in the bundle, which in fact reduces the fluctuations in the measurement time estimation errors as observed in Fig. 8.

The bundling of measurement data further reduces the number of message transmissions: For instance, if we bundle 10 measurement data in a “Report/Response” message (i.e.,  $N_{BM}=10$ ), we can reduce the number of message transmissions from 100 to 10, which is less than 0.3 percentage of the number of message transmissions for the schemes based on the conventional two-way message exchanges (i.e., 3,700).

Note that we need to be careful in interpreting the number of message transmissions as an indirect measure of energy consumption in this case. Because the bundling increases the length of message payload, the total number of bits transmitted for the case with the bundling is not the same as that for the case without the bundling given the number of messages. Still, however, the measurement bundling is an effective option to save the energy consumption because we can save the energy for the transmission of the overhead of a message including

a preamble, a frame header, and a frame check sequence by reducing the number of message transmissions. Also note that the measurement bundling can be used only when there are no strict timing requirements for the processing of measurement data due to the increased delay resulting from the bundling process.

#### IV. COMPARISON TO RELATED WORK

*Unsynchronized Clocks:* The proposed time synchronization scheme is similar to the *post-facto synchronization* scheme described in [17] in that sensor nodes’ clocks are unsynchronized and that the time of the occurrence of an event is first recorded with respect to the local clock. The difference is that time translation occurs at sensor nodes just after receiving synchronization messages from a “third-party” node (e.g., a head node) in the post-facto synchronization, while, in the proposed scheme, the time of the occurrence is transmitted to the head node without waiting for a synchronization message and the time translation is done at the head node. As for the receiver clock skew compensation, the use of network time protocol (NTP) [11] was suggested in [17]; because local-clock resolution and skew are minimized by the control-feedback design (e.g., based on phase-locked loop (PLL)), however, the NTP is not proper for low-power/complexity sensor nodes. In this regard the clock skew is handled by a one-way, low-complexity asynchronous SCFR scheme described in [9] for the proposed scheme.

*Reverse Two-Way Message Exchanges:* The ReversePTP proposed in [18] for time distribution in software defined networks (SDNs) is also similar to our work because the relationship and the direction of clock distribution between one master (i.e., the head node) and many slaves (i.e., sensor nodes) are reversed in both schemes. Their contexts (i.e., SDNs vs WSNs), however, are quite different from each other. As a consequence, the energy efficiency is not the main focus of the ReversePTP. For example, the slaves in the ReversePTP distribute their times to the master by periodically sending Sync messages. In the proposed scheme, it is the head node that distributes its time (i.e., clock frequency); if there is no data measurement, a sensor node does not transmit any message back to the head node for time synchronization.

*Passive Listening:* The idea of passive listening to time-stamped messages from other nodes is also discussed in [19] and [7]. The receiver-only synchronization (ROS) scheme proposed in [19] enables a subset of sensor nodes to achieve synchronization by overhearing the conventional two-way synchronization message exchanges of a pair of sensor nodes,



called *super nodes*; because of the additional information from the overheard two-way messages exchanges, the nodes can estimate both clock offset and clock skew without any message transmission. The application of ROS scheme, however, is limited to the sensor nodes located in the “Region of Pairwise Synchronization” where the messages from both super nodes can reach. Also, two super nodes performing two-way message exchanges are needed for ROS scheme.

The joint estimation algorithm based on prewhitening of observation models and least squares (LS) in [7] can be implemented either in a centralized or distributed ways, but the distributed approach incurs additional broadcast messages to distribute timestamps. In the proposed scheme, because the clock skew and offset estimation procedures are separated from each other, a distributed recursive algorithm can be applied for the clock skew estimation based on passive listening without incurring additional message broadcasting.

## V. CONCLUSIONS

In this paper we have proposed an energy-efficient time synchronization scheme for asymmetric WSNs, which is based on the asynchronous SCFR for one-way clock skew estimation/compensation at sensor nodes and reverse two-way message exchanges for clock offset estimation/translation at the head node in order to minimize the number of message transmissions at sensor nodes. Taking notice of the asymmetry between the head node and sensor nodes in terms of processing power and supplied energy, we move most of time synchronization operations to the head node in the proposed scheme and thereby reduce the complexity and power consumption of sensor nodes for time synchronization.

As for the one-way clock skew estimation/compensation, i.e., the only major operation to be done at sensor nodes, because the low complexity of the algorithm is critical for power efficiency, we use the CR estimator proposed in [9] for asynchronous SCFR, which is an unbiased estimator attaining the lower bound for a Gaussian delay as stated in Proposition 2. The comparative analysis presented in Section III-A shows that the CR estimator can provide relatively good performance with the lowest complexity among the estimators considered irrespective of the delay distribution. The simulation results in Section III-B in fact verifies that the proposed time synchronization scheme with the CR as the clock skew estimator provides the best performance in terms of the accuracy of measurement time estimation and, as an indirect measure of energy consumption, the number of message transmissions and receptions at a sensor node. In addition, if there are no strict timing requirements for the processing of measurement data, we can further reduce the number of message transmissions by bundling measurement data in a “Report/Response” message without significantly affecting the time synchronization performance, which is demonstrated by the simulation results in Section III-C.

Note that in this paper we have focused on the essential aspects of the proposed time synchronization scheme, i.e., the one-way clock skew estimation/compensation and the reverse two-way message exchanges combined with measurement data report messages, which leaves room for further extensions of

the proposed scheme; examples include the operations with multiple head nodes for redundancy and possibly localization as well [7] and the application of adaptive synchronization interval [2].

Of possible extensions, we have already shown how the proposed scheme can be extended to a hierarchical structure for network-wide, multi-hop synchronization through either simple packet-relaying or time-translating gateway nodes. The tradeoff between the complexity of gateway nodes and the performance of time synchronization for the two approaches is an important topic for further research and will be addressed in a followup work.

## APPENDIX A PROOF OF PROPOSITION 1

We first rephrase (9) as follows:

$$t_{a,i}(k) = R_i t_d(k) + \theta_i + d + n(k), \quad (17)$$

where  $d$  is a fixed portion of delay, which is assumed to be *known*, and  $n(k)$  is a random portion of delay following a zero-mean white Gaussian distribution with variance  $\sigma^2$ . From (17), we can construct a likelihood function and a log-likelihood function for the collective observation  $\mathbf{t}_{a,i} \triangleq \{t_{a,i}(j)\}_{j=0}^k$  and the parameters  $\theta_i$  and  $R_i$  as follows:

$$\begin{aligned} \mathcal{L}(\theta_i, R_i; \mathbf{t}_{a,i}) = & \\ & \prod_{j=1}^k \frac{1}{\sqrt{2\pi\sigma^2}} \exp\left(-\frac{(t_{a,i}(j) - (R_i t_d(j) + \theta_i + d))^2}{2\sigma^2}\right), \end{aligned} \quad (18)$$

and

$$\begin{aligned} \ln \mathcal{L}(\theta_i, R_i; \mathbf{t}_{a,i}) = & -\frac{k}{2} \ln(2\pi\sigma^2) \\ & - \frac{1}{2\sigma^2} \sum_{j=0}^k \{t_{a,i}(j) - (R_i t_d(j) + \theta_i + d)\}^2. \end{aligned} \quad (19)$$

Then the first derivatives of the log likelihood function with respect to  $\theta_i$  and  $R_i$  are given by

$$\begin{aligned} \frac{\partial \ln \mathcal{L}(\theta_i, R_i; \mathbf{t}_{a,i})}{\partial \theta_i} = & \\ & \frac{1}{\sigma^2} \sum_{j=0}^k \{t_{a,i}(j) - (R_i t_d(j) + \theta_i + d)\}, \end{aligned} \quad (20)$$

$$\begin{aligned} \frac{\partial \ln \mathcal{L}(\theta_i, R_i; \mathbf{t}_{a,i})}{\partial R_i} = & \\ & \frac{1}{\sigma^2} \sum_{j=0}^k t_d(j) \{t_{a,i}(j) - (R_i t_d(j) + \theta_i + d)\}. \end{aligned} \quad (21)$$

From (20) and (21), therefore, we obtain the joint one-way MLE of clock offset  $\hat{\theta}_i^{ML}(k)$  and skew  $\hat{R}_i^{ML}(k)$  as follows:

$$\hat{\theta}_i^{ML}(k) = \bar{t}_{a,i} - \hat{R}_i^{ML}(k) \bar{t}_d - d, \quad (22)$$

$$\hat{R}_i^{ML}(k) = \frac{\sum_{j=0}^k \{t_{a,i}(j) - (\hat{\theta}_i^{ML}(k) + d)\}}{\sum_{j=0}^k t_d^2(j)}. \quad (23)$$

After some manipulations, we can obtain closed-form expressions for  $\hat{\theta}_i^{ML}(k)$  and  $\hat{R}_i^{ML}(k)$  given in (10) and (11), respectively.

To obtain the CRLBs, we need the second derivatives of the log likelihood function with respect to  $\theta_i$  and  $R_i$ , which are given by

$$\frac{\partial^2 \ln \mathcal{L}(\theta_i, R_i; \mathbf{t}_{a,i})}{\partial \theta_i^2} = -\frac{k}{\sigma^2}, \quad (24)$$

$$\frac{\partial^2 \ln \mathcal{L}(\theta_i, R_i; \mathbf{t}_{a,i})}{\partial R_i^2} = -\frac{\sum_{j=0}^k t_d(j)^2}{\sigma^2} = -\frac{k}{\sigma^2} \bar{t}_d^2, \quad (25)$$

$$\frac{\partial^2 \ln \mathcal{L}(\theta_i, R_i; \mathbf{t}_{a,i})}{\partial \theta_i \partial R_i} = -\frac{\sum_{j=0}^k t_d(j)}{\sigma^2} = -\frac{k}{\sigma^2} \bar{t}_d. \quad (26)$$

Note that there is no need to take expectations because there are no terms related with  $t_{a,i}(j)$ . The Fisher information matrix in this case becomes

$$\mathbf{I}(\theta_i, R_i) = \frac{k}{\sigma^2} \begin{bmatrix} 1 & \bar{t}_d \\ \bar{t}_d & \bar{t}_d^2 \end{bmatrix}. \quad (27)$$

Because the CRLBs are the diagonal elements of the inverse of the Fisher information matrix [16, p. 40], we obtain

$$\mathbf{I}^{-1}(\theta_i, R_i) = \frac{\sigma^2}{k \left\{ \bar{t}_d^2 - (\bar{t}_d)^2 \right\}} \begin{bmatrix} \bar{t}_d^2 & -\bar{t}_d \\ -\bar{t}_d & 1 \end{bmatrix}. \quad (28)$$

From (28), therefore, we can obtain the CRLBs of clock offset and skew for the Gaussian delay model given in (12) and (13), i.e.,

$$\text{Var} \left( \hat{\theta}_i(k) \right) \geq \frac{\sigma^2 \cdot \bar{t}_d^2}{k \left\{ \bar{t}_d^2 - (\bar{t}_d)^2 \right\}},$$

$$\text{Var} \left( \hat{R}_i(k) \right) \geq \frac{\sigma^2}{k \left\{ \bar{t}_d^2 - (\bar{t}_d)^2 \right\}}.$$

Note that the joint MLEs of clock offset  $\hat{\theta}_i^{ML}(k)$  and skew  $\hat{R}_i^{ML}(k)$  are *efficient estimators*: First, from (11), we obtain

$$\mathbb{E} \left[ \hat{R}_i^{ML}(k) \right] = \frac{\mathbb{E} [t_d t_{a,i}] - \bar{t}_d \mathbb{E} [t_{a,i}]}{\bar{t}_d^2 - (\bar{t}_d)^2}. \quad (29)$$

From (17), we have

$$\mathbb{E} [\bar{t}_d t_{a,i}] = R_i \bar{t}_d^2 + (\theta_i + d) \bar{t}_d, \quad (30)$$

$$\mathbb{E} [\bar{t}_{a,i}] = R_i \bar{t}_d + (\theta_i + d). \quad (31)$$

Inserting (30) and (31) into (29), we obtain  $\mathbb{E} [\hat{R}_i^{ML}(k)] = R_i$ , which shows that  $\hat{R}_i^{ML}(k)$  is an unbiased estimator.

Secondly, from (11), we also obtain

$$\text{Var} \left( \hat{R}_i^{ML}(k) \right) = \frac{\text{Var} (\bar{t}_d t_{a,i}) - (\bar{t}_d)^2 \text{Var} (\bar{t}_{a,i})}{\left\{ \bar{t}_d^2 - (\bar{t}_d)^2 \right\}^2}. \quad (32)$$

From (17), we have

$$\text{Var} (\bar{t}_d t_{a,i}) = \frac{\sum_{j=0}^k t_d(j)^2 \text{Var} (n(k))}{k^2} = \frac{\sigma^2}{k} \bar{t}_d^2, \quad (33)$$

$$\text{Var} (\bar{t}_{a,i}) = \frac{\sum_{j=0}^k \sigma^2}{k^2} = \frac{\sigma^2}{k}. \quad (34)$$

Inserting (33) and (34) into (32), we obtain

$$\text{Var} \left( \hat{R}_i^{ML}(k) \right) = \frac{\sigma^2}{k \left\{ \bar{t}_d^2 - (\bar{t}_d)^2 \right\}},$$

which is the CRLB in (13). Similar procedures can be taken for  $\hat{\theta}_i^{ML}(k)$  to show that it is also an efficient estimator. ■

## APPENDIX B PROOF OF PROPOSITION 2

It is straightforward to see that  $\hat{R}_i^{CR}(k)$  is unbiased because

$$\mathbb{E} \left[ \hat{R}_i^{CR}(k) \right] = \mathbb{E} \left[ R_i + \frac{1}{\bar{t}_d(k)} \tilde{d}(k) \right] = R_i. \quad (35)$$

As for the variance, we first construct from (14) a likelihood function for the observation  $\tilde{t}_{a,i}(k)$  and the parameter  $R_i$ :

$$\mathcal{L}(R_i; \tilde{t}_{a,i}(k)) = \frac{1}{\sqrt{4\pi\sigma^2}} \exp \left( -\frac{(\tilde{t}_{a,i}(k) - R_i \tilde{t}_d(k))^2}{4\sigma^2} \right). \quad (36)$$

Then the first and the second derivatives of the log likelihood function are given by

$$\frac{\partial \ln \mathcal{L}(R_i; \tilde{t}_{a,i}(k))}{\partial R_i} = \frac{\tilde{t}_{a,i}(k) - R_i \tilde{t}_d(k)}{2\sigma^2} \tilde{t}_d(k), \quad (37)$$

$$\frac{\partial^2 \ln \mathcal{L}(R_i; \tilde{t}_{a,i}(k))}{\partial^2 R_i} = -\frac{\tilde{t}_d(k)^2}{2\sigma^2}. \quad (38)$$

From (37), we can see that  $\hat{R}_i^{CR}(k)$  is in fact the estimator maximizing the log-likelihood function. Also from (38), applying the same steps to derive a CRLB, we can obtain the lower bound of clock skew as follows

$$\text{Var} \left( \hat{R}_i^{CR}(k) \right) \geq \frac{2\sigma^2}{\tilde{t}_d(k)^2}. \quad (39)$$

Because the variance of  $\hat{R}_i^{CR}(k)$  is given by

$$\text{Var} \left( \hat{R}_i^{CR}(k) \right) = \text{Var} \left( R_i + \frac{\tilde{d}(k)}{\tilde{t}_d(k)} \right) = \frac{2\sigma^2}{\tilde{t}_d(k)^2}, \quad (40)$$

$\hat{R}_i^{CR}(k)$  attains the lower bound given by (39). ■

## REFERENCES

- [1] Y.-C. Wu, Q. Chaudhari, and E. Serpedin, "Clock synchronization of wireless sensor networks," *IEEE Signal Process. Mag.*, vol. 28, no. 1, pp. 124–138, 2011.
- [2] M. Akhlaq and T. R. Sheltami, "RTSP: An accurate and energy-efficient protocol for clock synchronization in WSNs," *IEEE Trans. Instrum. Meas.*, vol. 62, no. 3, pp. 578–589, Mar. 2013.
- [3] D. Macii, A. Ageev, and A. Somov, "Power consumption reduction in wireless sensor networks through optimal synchronization," in *Proc. I2MTC '09*, May 2009, pp. 1346–1351.
- [4] J. Elson, L. Girod, and D. Estrin, "Fine-grained network time synchronization using reference broadcasts," in *Proc. of 5th Symp. Operating System Design and Implementation*, Dec. 2002, pp. 147–163.
- [5] T. Trump, "Maximum likelihood trend estimation in exponential noise," *IEEE Trans. Signal Process.*, vol. 49, no. 9, pp. 2087–2095, Sep. 2001.
- [6] R. T. Rajan and A.-J. van der Veen, "Joint ranging and clock synchronization for a wireless network," in *Proc. of CAMSAP 2011*, Dec. 2011, pp. 297–300.
- [7] S. P. Chepuri, R. T. Rajan, G. Leus, and A.-J. van der Veen, "Joint clock synchronization and ranging: Asymmetrical time-stamping and passive listening," *IEEE Signal Process. Lett.*, vol. 20, no. 1, pp. 51–54, Jan. 2013.
- [8] S. B. Moon, P. Skelly, and D. Towsley, "Estimation and removal of clock skew from network delay measurements," in *Proc. 1999 IEEE INFOCOM*, New York, NY, Mar. 1999.
- [9] K. S. Kim, "Asynchronous source clock frequency recovery through aperiodic packet streams," *IEEE Commun. Lett.*, vol. 17, no. 7, pp. 1455–1458, Jul. 2013.
- [10] A. Mainwaring, J. P. R. Szewczyk, D. Culler, and J. Anderson, "Wireless sensor networks for habitat monitoring," in *Proc. WSNA '02*. New York, NY, USA: ACM, 2002, pp. 88–97.
- [11] D. L. Mills, "Internet time synchronization: The network time protocol," *IEEE Trans. Commun.*, vol. 39, no. 10, pp. 1482–1493, Oct. 1991.
- [12] S. Ganeriwal, R. Kumar, and M. B. Srivastava, "Timing-sync protocol for sensor networks," in *Proc. SenSys'03*. New York, NY, USA: ACM, 2003, pp. 138–149.
- [13] K. S. Kim, "Comments on "ieee 1588 clock synchronization using dual slave clocks in a slave"," *IEEE Commun. Lett.*, vol. 18, no. 6, pp. 981–982, Jun. 2014.
- [14] K.-L. Noh, Q. M. Chaudhari, E. Serpedin, and B. W. Suter, "Novel clock phase offset and skew estimation using two-way timing message exchanges for wireless sensor networks," *IEEE Trans. Commun.*, vol. 55, no. 4, pp. 766–777, Apr. 2007.
- [15] A. Guchhait and R. M. Karthik, "Joint minimum variance unbiased and maximum likelihood estimation of clock offset and skew in one-way packet transmission," in *Proc. IEEE 81st Vehicular Technology Conference (VTC2015-Spring)*, May 2015, pp. 1–6.
- [16] S. M. Kay, *Fundamentals of statistical signal processing: Estimation theory*. Upper Saddle River, NJ, USA: Prentice-Hall, Inc., 1993, vol. 1.
- [17] J. Elson and D. Estrin, "Time synchronization for wireless sensor networks," in *Proc. IPDPS 2001*, San Francisco, CA, USA, Apr. 2001.
- [18] T. Mizrahi and Y. Moses, "Using reverseptp to distribute time in software defined networks," in *Proc. of ISPCS 2014*, Sep. 2014, pp. 112–117.
- [19] N. Kyoung-lae and E. Serpedin, "Pairwise broadcast clock synchronization for wireless sensor networks," in *Proc. WoWMoM 2007*, Jun. 2007, pp. 1–6.